

## Supporting Information

### Probing metabolic alterations in breast cancer in response to molecular inhibitors with Raman spectroscopy and validated with mass spectrometry†

Xiaona Wen,<sup>‡a</sup> Yu-Chuan Ou,<sup>‡a</sup> Galina Bogatcheva,<sup>b</sup> Giju Thomas,<sup>c</sup> Anita Mahadevan-Jansen,<sup>c</sup> Bhuminder Singh,<sup>b</sup> Eugene C. Lin,<sup>d</sup> and Rizia Bardhan<sup>ef\*</sup>

<sup>a</sup>Department of Chemical and Biomolecular Engineering, Vanderbilt University, Nashville, TN 37235, USA

<sup>b</sup>Department of Medicine, Vanderbilt University Medical Center, Nashville, TN 37232, USA

<sup>c</sup>Vanderbilt Biophotonics Center, Vanderbilt University, Nashville, TN 37232, USA

<sup>d</sup>Department of Chemistry and Biochemistry, National Chung Cheng University, Chiayi 62106, Taiwan

<sup>e</sup>Department of Chemical and Biological Engineering, Iowa State University, Ames, IA 50012, USA

<sup>f</sup>Nanovaccine Institute, Iowa State University, Ames, IA 50012, USA

\*Corresponding Author

E-mail: [rbardhan@iastate.edu](mailto:rbardhan@iastate.edu)

† Electronic supplementary information (ESI) available.

‡ Authors contributed equally.

### Table of Contents

- p. S2: Fig. S1** Representative Raman spatial maps.
- p. S3: Fig. S2** Examples of individual spectrum for the Raman map acquired from each MDA-MB-231 cell before and after smoothing and background subtraction.
- p. S3: Fig. S3** Selective Raman peaks changed post-treatment with Trametinib.
- p. S4: Fig. S4** PC loading of MDA-MB-231 cells treated with various concentrations of Trametinib relative to untreated cells.
- p. S5: Fig. S5** Ratiometric analysis of metabolites for MDA-MB-231 cells treated with various concentrations of Trametinib relative to untreated cells.
- p. S6: Fig. S6** MDA-MB-231 cells treated with Alpelisib and interrogated with RS.
- p. S6: Fig. S7** RS distinguishing responders from nonresponders as a function of drug type.
- p. S7: Fig. S8** Comparison of MDA-MB-231 cells treated with mono- or combination therapy.
- p. S8: Fig. S9** Examples of individual spectrum for the Raman map acquired from each MCF-7 cell before and after smoothing and background subtraction.
- p. S9: Fig. S10** PC loading of MCF-7 cells treated with various concentrations of Trametinib relative to untreated cells.

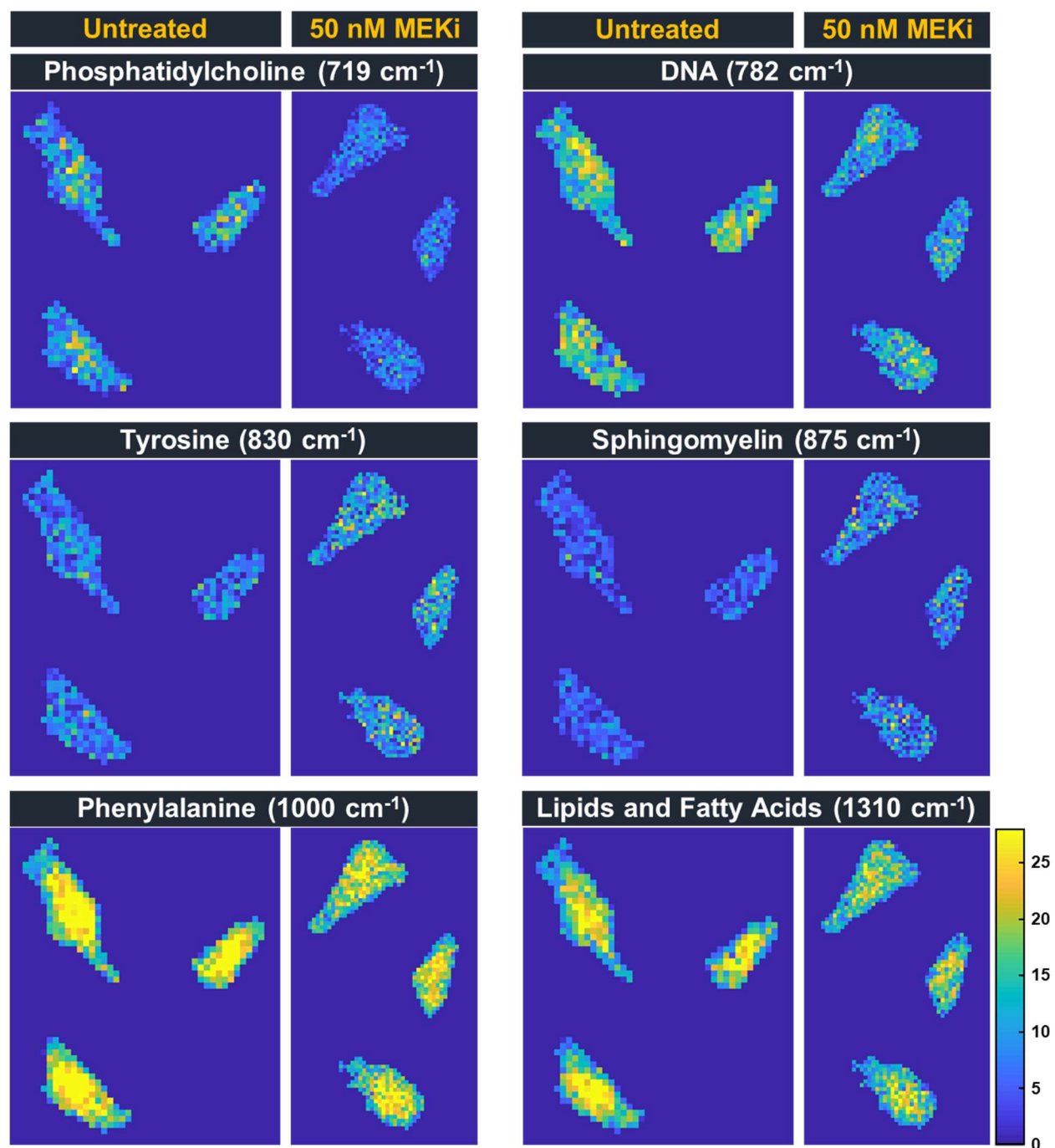


**Fig. S1** Representative Raman spatial maps of untreated MDA-MB-231 cells and those treated with MEKi (Trametinib, 50 nM) shown at 719  $\text{cm}^{-1}$  (phosphatidylcholine), 782  $\text{cm}^{-1}$  (DNA), 830  $\text{cm}^{-1}$  (tyrosine), 875  $\text{cm}^{-1}$  (sphingomyelin), 1000  $\text{cm}^{-1}$  (phenylalanine) and 1310  $\text{cm}^{-1}$  (lipids and fatty acids). The corresponding spectra and quantification of these peaks before and after treatment are shown in Fig. 1a and c in the main text. Raman intensity decreased post-treatment at 719, 782, 1000, and 1310  $\text{cm}^{-1}$ , but increased post-treatment at 830, and 875  $\text{cm}^{-1}$ .

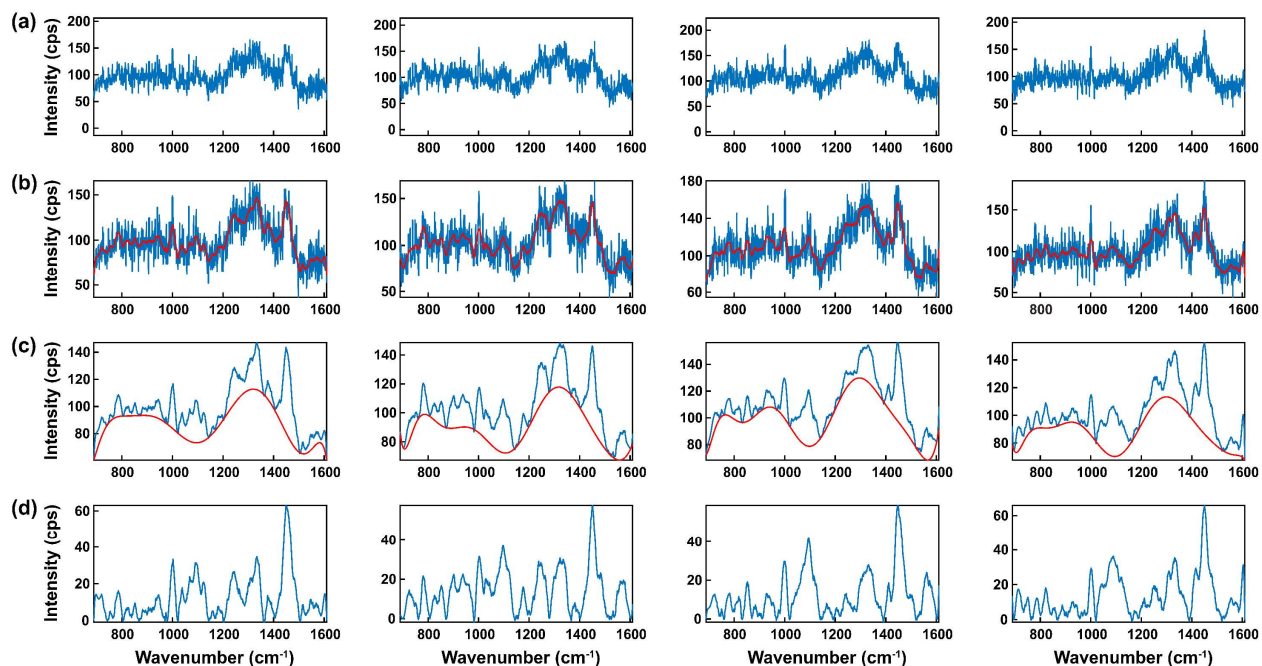


**Fig. S2** Examples of individual spectrum for the Raman map acquired from each MDA-MB-231 cell. (a) Representative raw Raman spectra. (b) The raw spectra were smoothed (Savitzky-Golay, fifth-order polynomial, 47 points). (c) The spectra were then baseline corrected (11<sup>th</sup>-order polynomial, 0.0001 threshold). (d) The spectra after smoothing and baseline correction.

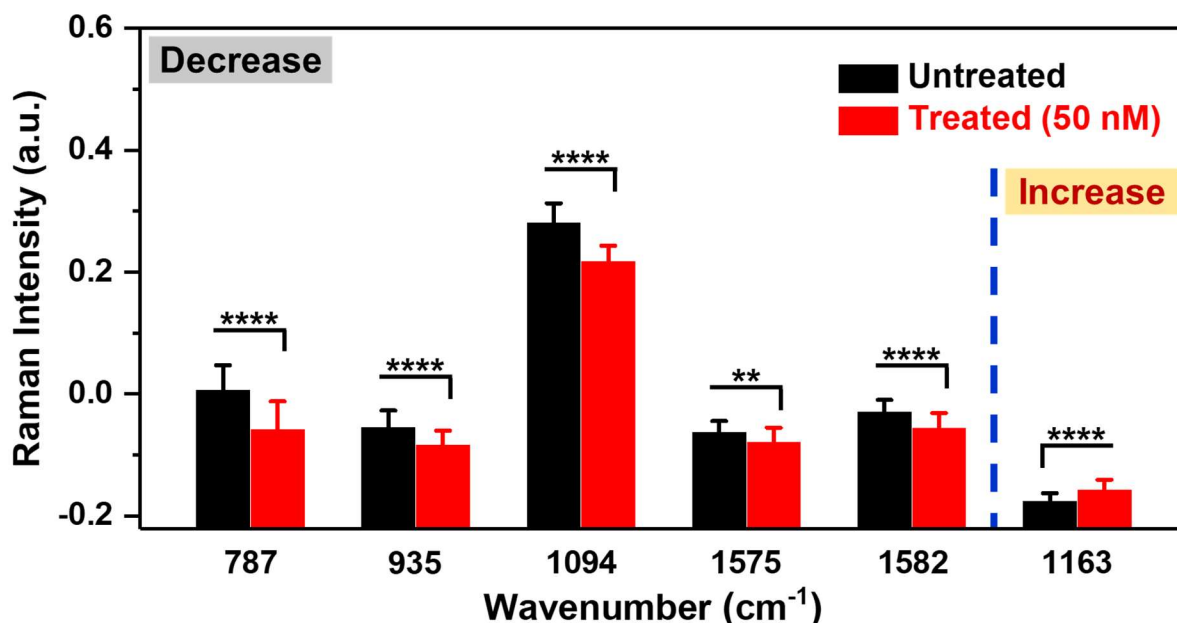


**Fig. S3** MDA-MB-231 cells treated with Trametinib and probed with RS. Selective Raman peaks that decreased with treatment including phosphatidylserine (787 cm<sup>-1</sup>), proteins and amino acids (935 cm<sup>-1</sup>), DNA (1094 and 1575 cm<sup>-1</sup>) and phenylalanine (1582 cm<sup>-1</sup>). Selective Raman peak that increased after treatment including tyrosine (1163 cm<sup>-1</sup>). Here, \*\* indicates  $p < 0.01$  and \*\*\*\* indicates  $p < 0.0001$  determined by student's t-test.

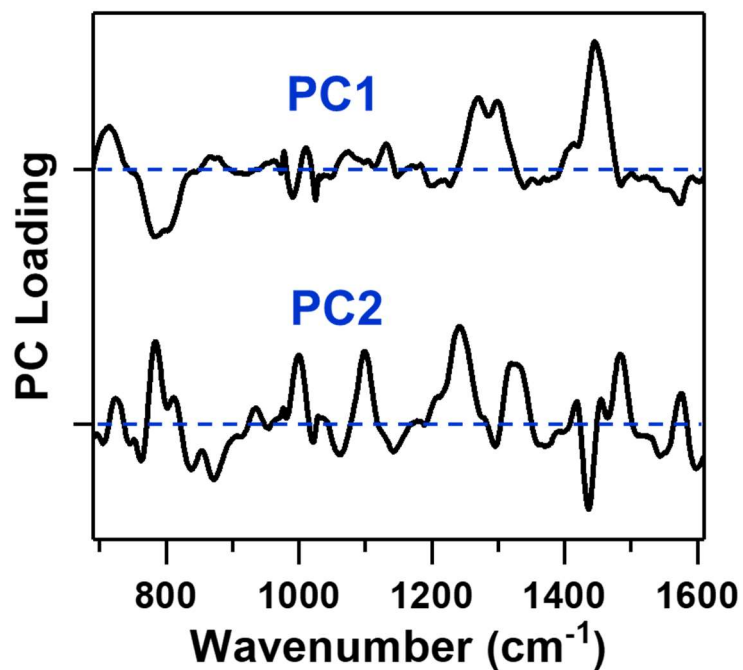


**Fig. S4** PC loading of MDA-MB-231 cells treated with various concentrations of Trametinib (1, 50 and 300 nM) relative to untreated cells. The corresponding PC scatter plot is shown in Fig. 2b. The features in both PC1 and PC2 generally correlated well to the PC loading shown in Fig. 1e that is the simplest case only comparing untreated cells to those treated with Trametinib at its working concentration (50 nM).

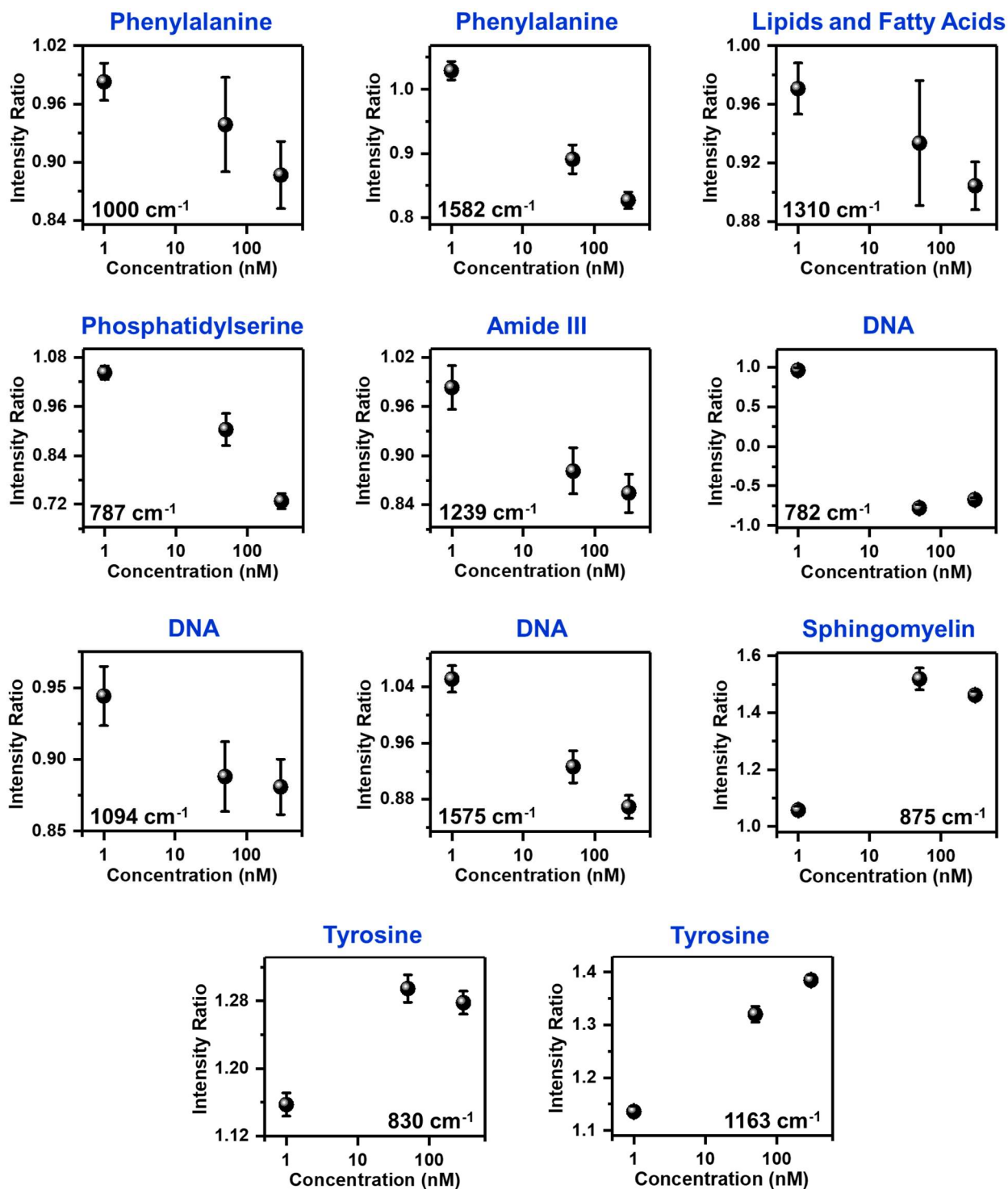


**Fig. S5** Ratiometric analysis of metabolites by examining changes in Raman footprint when MDA-MB-231 cells were treated with various concentrations of Trametinib (1, 50 and 300 nM) compared with untreated cells. Several metabolites decreased and some increased post-treatment.

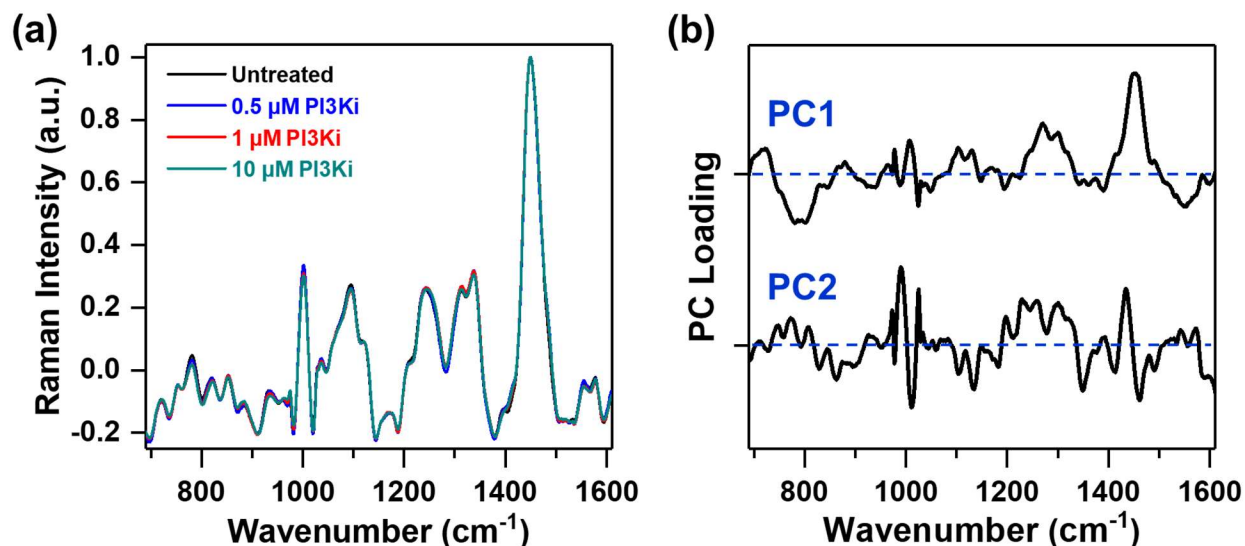


**Fig. S6** MDA-MB-231 cells treated with Alpelisib and interrogated with RS. (a) Mean normalized Raman spectra of untreated MDA-MB-231 cells and those treated with various concentrations (0.5, 1 and 10  $\mu\text{M}$ ) of PI3Ki (Alpelisib). Spectra were normalized to 1440  $\text{cm}^{-1}$  biological peak. (b) PC loading of MDA-MB-231 cells treated with various concentrations of Alpelisib relative to untreated cells. The corresponding PC scatter plot is shown in Fig. 3a.

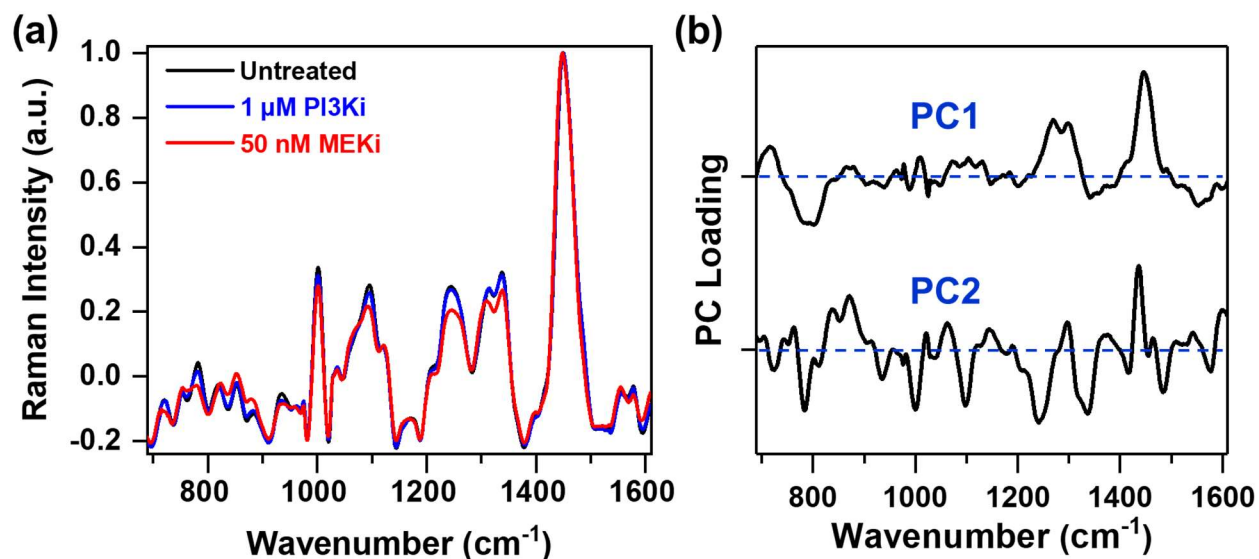


**Fig. S7** RS distinguishing responders from nonresponders as a function of drug type. (a) Mean normalized Raman spectra of untreated MDA-MB-231 cells and those treated with MEKi (Trametinib) or PI3Ki (Alpelisib). Spectra were normalized to 1440  $\text{cm}^{-1}$  biological peak. (b) PC loading of MDA-MB-231 cells treated with MEKi (Trametinib) or PI3Ki (Alpelisib) relative to untreated cells. The corresponding PC scatter plot is shown in Fig. 3b.



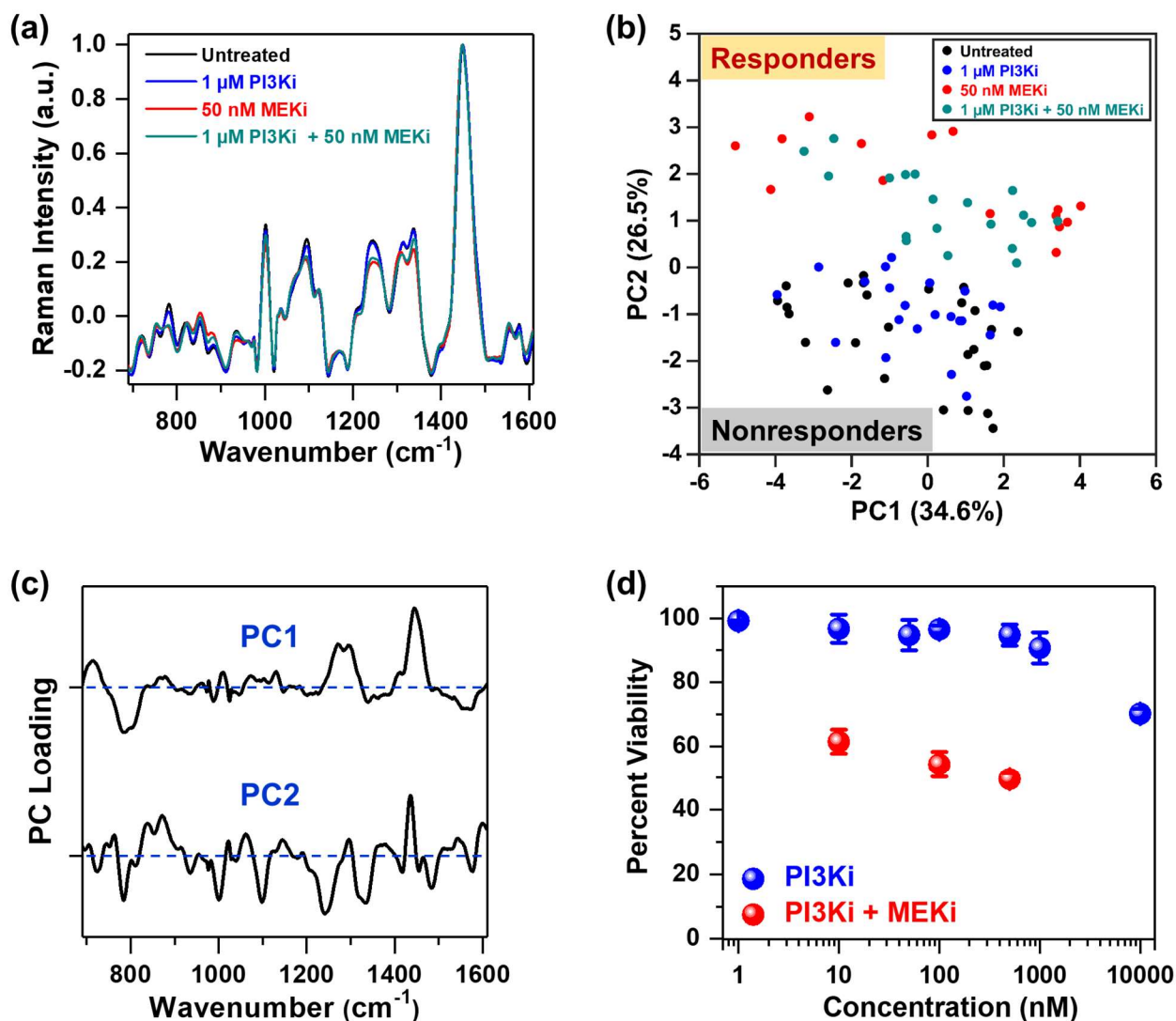


**Fig. S8** Comparison of MDA-MB-231 cells treated with mono- or combination therapy. (a) Mean normalized Raman spectra of untreated cells (black) and cells treated with PI3Ki (Alpelisib, 1  $\mu$ M, blue), MEKi (Trametinib, 50 nM, red), and combination treatment (1  $\mu$ M PI3Ki + 50 nM MEKi, cyan). Spectra were normalized to 1440  $\text{cm}^{-1}$  biological peak. (b) Corresponding PCA scatter plot. Clear clustering of cells was observed for cells that were responsive to treatment vs. nonresponsive. (c) PC loading of (b). (d) Cell viability assay comparing cells treated with PI3Ki (Alpelisib) at various concentrations, relative to combination treatment where the concentration of Trametinib was kept constant at 50 nM and that of Alpelisib was varied (10, 100 and 500 nM,  $n = 4$  for each concentration). Cell viability was measured by a plate reader at 540 nm. All data were presented as mean  $\pm$  standard deviation.

We investigated the impact of combinatorial treatment combining MEKi (Trametinib) and PI3Ki (Alpelisib) due to the strong evidence of convergence and crosstalk between the PI3K/AKT/mTOR and Ras/Raf/MEK/ERK pathways that control oncogenic signaling.<sup>1,2</sup>

Numerous clinical trials (NCT01347866, NCT01337765, NCT01390818, *etc.*) are currently underway to investigate the feasibility and efficacy of MEK and PI3K dual inhibition. We observed that the responders were differentiated from nonresponders in PCA where the cells treated with combination treatment clustered with those treated with Trametinib alone. The cells in the combination treatment groups did not differentiate from the monotherapy group. These observations implied that further experiments would be necessary with RS and MS to explore the complex changes in metabolic pathways after combination treatment. Further, PCA may not be sufficient in assessing results from combination treatments, and more advanced machine learning algorithms may be necessary.<sup>3</sup>

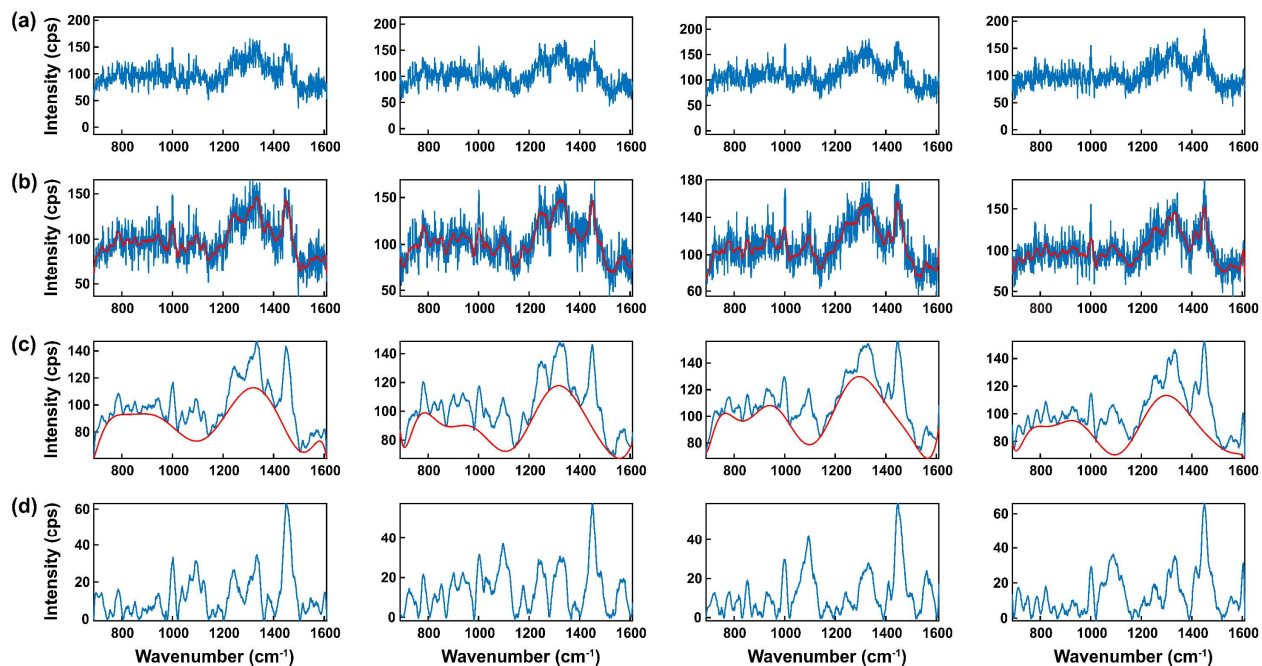


**Fig. S9** Examples of individual spectrum for the Raman map acquired from each MCF-7 cell. (a) Representative raw Raman spectra. (b) The raw spectra were smoothed (Savitzsky-Golay, fifth-order polynomial, 47 points). (c) The spectra were then baseline corrected (11<sup>th</sup>-order polynomial, 0.0001 threshold). (d) The spectra after smoothing and baseline correction.



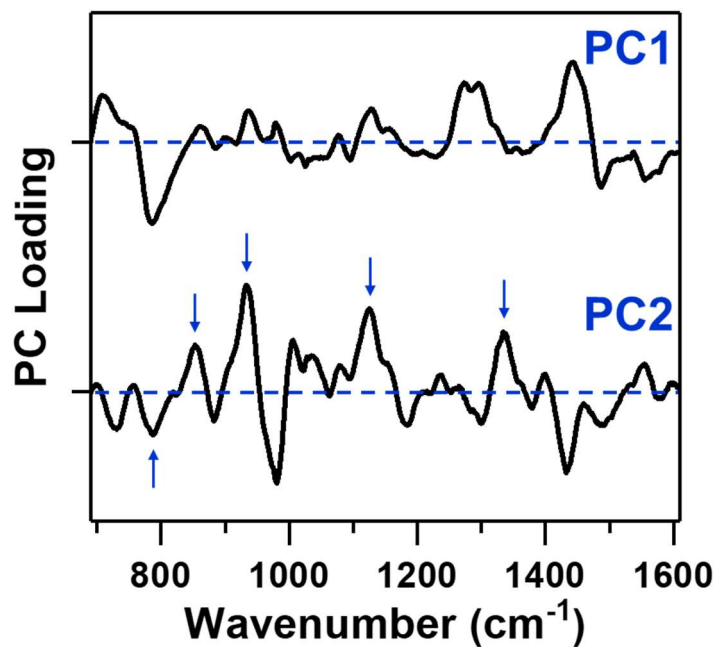


**Fig. S10** PC loading of MCF-7 cells treated with various concentrations of MEKi (Trametinib) relative to untreated cells. The corresponding PC scatter plot is shown in Fig. 5b.

## References

- 1 M. C. Mendoza, E. E. Er and J. Blenis, *Trends Biochem. Sci.*, 2011, **36**, 320-328.
- 2 Z. Cao, Q. Liao, M. Su, K. Huang, J. Jin and D. Cao, *Cancer Lett.*, 2019, **459**, 30-40.
- 3 S. L. Goldenberg, G. Nir and S. E. Salcudean, *Nat. Rev. Urol.*, 2019, **16**, 391-403.